3D-Mirrorcle: Bridging the Virtual and Real through Depth Alignment in AR Mirror Systems

YUJIA LIU, Tsinghua University, China
QI XIN, Tsinghua University, China
CHENZHUO XIANG, Tsinghua University, China
YU ZHANG, Tsinghua University, China
XUHAI XU, Columbia University, USA
YINGQING XU, Tsinghua University, China

(a) (b)

Fig. 1. 3D-Mirrorcle is a smart mirror that overlays augmented reality (AR) with depth perception on a mirror surface. (a) System structure: it employs lenticular gratings between the screen and half-mirror, and adopts depth alignment and segmentation algorithms to project separate images to each eye, merging into a 3D display for an immersive mirror AR experience. (b) Example applications: facial massage and body posture guidance.

Smart mirrors have emerged as a novel augmented reality (AR) interface in home environments. However, due to the binocular disparity in human vision, one major challenge is the depth mismatch between the 3D mirror reflection and the 2D screen display. This disparity can cause the display content to appear as if it's floating above the mirror, disrupting the seamless integration of the two components and hindering the overall usability of the smart mirrors. In this study, we introduce 3D-Mirrorcle, an AR mirror system that addresses this issue through a synergistic hardware-software co-design on a lenticular grating setup. Unlike previous works that require bulky devices or shutter glasses, with our implemented real-time position adjustment and depth adaptation algorithms, the screen display can be dynamically aligned to the user's depth perception for a realistic and immersive experience. Our user study (N=24) indicates that 3D-Mirrorcle show significant improvements in task accuracy (49.66% ↑), task completion time (35.49%

Manuscript submitted to ACM

↓), immersion (74.07% ↑), and usability (11.94% ↑), thereby boosting overall user satisfaction in comparison to existing baselines. We envision our system as a transformative leap in mirror-based AR experiences, with the potential to unlock new software markets for industries like education, healthcare, and beyond.

CCS Concepts: • **Human-centered computing → Visualization systems and tools**; **Mixed / augmented reality**; • **Hardware → Displays and imagers**.

Additional Key Words and Phrases: Augmented Reality, Smart Mirror, Parallax, Depth Alignment

ACM Reference Format:
Yujia Liu, Qi Xin, Chenzhuo Xiang, Yu Zhang, Xuhai Xu, and Yingqing Xu. 2024. 3D-Mirrorcle: Bridging the Virtual and Real through Depth Alignment in AR Mirror Systems. In . ACM, New York, NY, USA, 19 pages. https://doi.org/XXXXXXX.XXXXXXX

1 INTRODUCTION

The recent advancement of Augmented Reality (AR) technology presents immense potential for the creation of novel applications across domains [9, 38]. An ideal AR interface should seamlessly integrate into the real world without requiring bulky wearables [31, 61, 62]. Despite these advancements, practical implementations of AR still face substantial limitations. Smartphone-based AR systems, for example, are constrained by small screen sizes and limited camera capabilities [68], while AR glasses often require conspicuous equipment that may deter widespread adoption [69].

Mirrors, which naturally reflect depth, not only preserve the authenticity of the real environment but also introduce an additional dimension, blending reality with virtual enhancements. This capability has elevated smart mirrors as a promising AR interface within smart home settings. These mirrors, augmented with digital displays, are now employed in various domains including fitness guidance [2, 24], virtual garment fitting [18, 20], personal hygiene [39, 48, 54], and emotional well-being [4, 13, 66, 67]. Two primary methods have emerged for integrating AR into mirror interfaces. The first involves simulating mirrors using cameras and displays, though this method suffers from low resolution, limited depth perception, and unnatural viewing angles [46]. The second method combines the display with a half-mirror, a partially reflective mirror that simultaneously transmits and reflects light, thus merging reflective properties with digital content more seamlessly [1, 3, 10, 19].

However, challenges arise with the second method when considering the human visual system, which uses slight differences in observation angles to perceive depth—a phenomenon known as "binocular disparity" or "parallax" (see Figure 2.a) [12]. Directly placing a half-mirror on the screen can lead to a depth mismatch, where the 2D screen content appears to float above the mirror surface, significantly degrading user experience (see Figure 2.b). Previous attempts to resolve this issue have involved setting the screen at a specific distance behind the half-mirror to align the perceived depth [5, 14, 21, 23, 47, 57], or incorporating projectors at various system locations [8, 40] to achieve depth perception. These methods, however, fix the depth at a constant value and require users to maintain a steady distance from the mirror, limiting their practical daily use.

To bridge the research gaps, we developed **3D-Mirrorcle**, a compact AI-powered mirror display system that dynamically adjusts visual depth, providing a natural 3D perception of virtual objects in the mirror (see Figure 1). It affixes a lenticular grating [32–34] to a 2D screen that allows each human eye to see different parts of the image, thereby creating depth perception. As depicted in Figure 2.c, the human brain can perceive an object behind the screen at a certain depth when the left and right eye views are appropriately offset.

Most importantly, 3D-Mirrorcle tracks users' eye positions in real-time and can adjust depth dynamically without the need for additional wearable devices, which expands the possibilities for a diverse array of real-world applications.

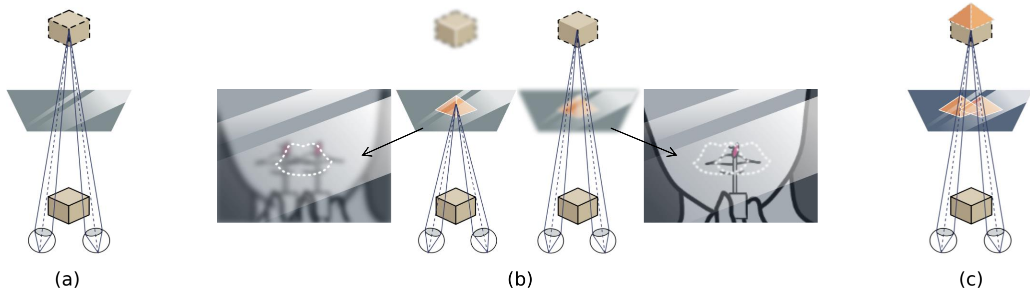

Fig. 2. (a) Parallax in human vision. (b) Depth mismatch in 2D smart mirrors: the mirror reflection blurs when viewing the screen display, and the screen blurs vice versa. (c) Two separate images are displayed for each eye to achieve depth perception.

By co-designing hardware and software altogether, our system enables a natural and immersive augmented reality experience within the mirror space.

We evaluated 3D-Mirrorcle through four tasks, divided into standardized and application categories, with extensive user studies involving 24 participants. The standardized tasks — facial and air outlining — assess task completion quality, where 3D-Mirrorcle surpasses existing 2D smart mirrors and video-based mirrors by achieving up to 49.66% greater accuracy and 35.49% improved efficiency. Application tasks, designed to simulate everyday scenarios like facial massage and fitness exercises, demonstrated 3D-Mirrorcle's practical usability. Specifically, 3D-Mirrorcle scored a System Usability Scale (SUS) average of 71.61, significantly outperforming the 2D smart mirror (65.36) and video-based mirror (66.35), with an enhancement in immersion by up to 74.07%, reflecting a deeper user engagement with the system. Despite the increased mental demand reported in our NASA-TLX evaluation, 3D-Mirrorcle demonstrated superior performance across the tasks. Users experienced greater overall satisfaction, confirming 3D-Mirrorcle's enhanced effectiveness and usability in both standardized tasks and real-world applications compared to existing smart mirror systems.

The key contributions of our paper can be summarized as follows:

(1) We introduced 3D-Mirrorcle, an innovative 3D AR mirror system that dynamically presents 3D virtual perceptions in the mirror space through real-time mirror reflection alignment and lenticular grating segmentation.
(2) We conducted comprehensive user studies to demonstrate 3D-Mirrorcle's advantages in task accuracy, time efficiency, immersion, usability, and overall user satisfaction, setting a new standard for mirror AR solutions.

2 RELATED WORK

This section provides an overview of existing research on AR in mirror space and 3D display technologies.

2.1 AR in Mirror

There has been extensive research on displaying AR content in the mirror space. Traditional video-based interfaces used front-facing cameras and screens to blend real and virtual elements for anatomical education [6], motion training [2], conductors' practice [50], and stimulate laughter [41]. However, unlike optical mirrors, the video stream displayed in these systems suffers from issues like lower resolution, changed perspectives, depth loss, lack of direct eye contact, and delays, making the interaction less realistic [46].

System	Hardware	Real Mirror	Consistent Viewpoint	Dynamic Depth	Glasses-Free Interaction	Daily-use Practicality
Video-based [46]	Camera + video stream		✓		✓	✓
2D-Optical [3]	2D display + half-mirror	✓			✓	✓
Depth-aligned [40]	2D display + half-mirror at specific distance	✓	✓		✓	
3D-Optical [32, 33]	3D display + half-mirror + shutter glasses	✓	✓	✓		
3D-Mirrorcle	3D display + half-mirror	✓	✓	✓	✓	✓

Table 1. Comparison among smart mirror systems. Systems that do not support user interaction, such as the grating-based prototype discussed in Lee et al. [32, 33], are excluded from this comparison.

To preserve the properties of optical mirrors, another approach involves attaching half-mirrors to screens. This setup is prevalent in smart mirrors within IoT scenarios to display information [1, 3, 10, 19] and in fields like fitness [4, 24], psychological therapy [42], and fashion [35]. However, these 2D-optical mirror systems fail to seamlessly integrate AR due to depth mismatches; the content appears only on the mirror's surface without any depth perception, leading to poor immersion in user experience.

In response, some research has focused on enhancing depth perception in AR by positioning half-mirrors at specific distances or angles from the display [14, 21, 23, 47, 57] or by adjusting projectors [8, 40]. These systems, however, require users to maintain a fixed distance from the mirror, which is impractical for everyday use.

As 3D display technology advances, recent works have employed gratings on transparent screens [34] or between the screen and mirror [32, 33] for autostereoscopic 3D displays. Nevertheless, these technologies do not support interaction with user's body, and they lack user evaluations [33]. Despite their adoption of shutter glasses as a workaround, such a system does not support a natural glasses-free mirror interaction, which hinders its application in the real world.

In contrast, 3D-Mirrorcle effectively leverages grating technology to enable glasses-free AR displays with dynamic depth adjustment based on user movement, making it suitable for daily mirror use. The major differences among current smart mirror systems are summarized in Table 1.

2.2 3D Display

When viewing objects, people combine the images seen by each eye, and the brain processes the binocular disparity to perceive depth, forming the biological foundation of 3D display technology [49].

Accordingly, 3D visuals can be created by generating differential images for each eye through various methods, broadly categorized into three types [17, 56]: stereoscopic direct-view (requiring glasses), head-mounted and interactive (involving wearable digital devices), and autostereoscopic direct-view (glasses-free). The first two types require equipment that may not be readily available in everyday settings, while glasses-free methods offer greater convenience as they do not require special wearables.

Among glasses-free systems, various approaches include reflection-based [64], diffraction-based [30, 55], and projection-based methods [11, 29]. However, these techniques often demand considerable space. Therefore, our focus will be on the more space-efficient occlusion and refraction-based methods.

The occlusion-based method utilizes a parallax barrier placed at a specific distance from the display, enabling each eye to see different parts of the image [28, 65]. This method, however, can reduce brightness and pixel density and cause crosstalk—where images intended for one eye are seen by the other—particularly if the aperture is narrowed to improve light efficiency.

Conversely, the refraction-based method employs a lenticular grating on the screen to direct light from pixels to be viewed from certain angles, thus facilitating a 3D effect. Despite its advantages, this method also faces challenges such as reduced brightness and resolution, along with similar crosstalk issues. Some improvements have been made

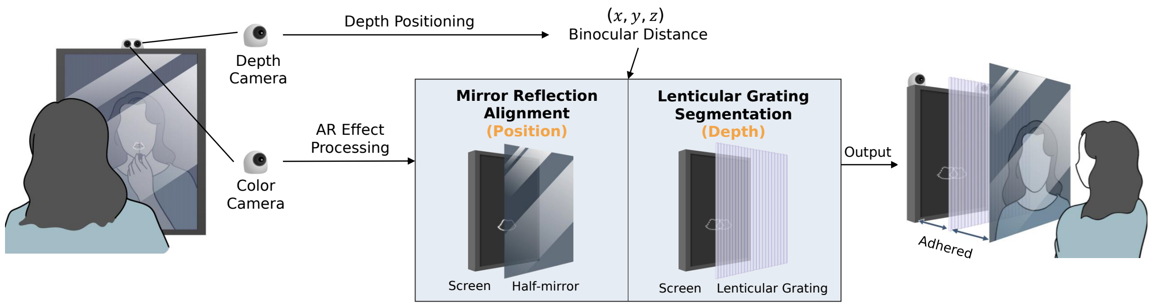

Fig. 3. Pipeline of 3D-Mirrorcle: Eye coordinates are first located using a depth camera, while facial and body key points are identified via a color camera. The display processes these inputs to create AR effects, incorporating position alignment and lenticular grating segmentation. This setup enables viewers to see both their reflections and the augmented content clearly on the display.

by tilting the lens structure for horizontal and vertical distribution [58, 59]. Further innovations include techniques for 360-degree 3D imaging [15] and eye position-dependent image generation [25, 27, 43–45, 51, 53].

3D-Mirrorcle adopts the space-efficient refraction-based method with self-adaptive reflection alignment and segmentation algorithms, enabling interactive 3D displays on a mirror surface. Its system implementation is grounded in the mature 3D display technology of the Leia Lume Pad 2 [16].

3 3D-MIRRORCLE

3D-Mirrorcle is a smart mirror system that integrates hardware and software to deliver immersive AR content on a mirror surface that dynamically adapts to users' movements for natural interaction. Figure 3 illustrates the system's pipeline.

Specifically, the hardware of 3D-Mirrorcle consists of three layers: a half-mirror, lenticular grating, and a display screen, assembled tightly without any gaps. A depth camera captures the user's eye coordinates, and a color camera captures images for facial and body recognition and subsequent AR effect processing. On the software side, two key algorithms are adopted to enhance user experience: the *Mirror Reflection Alignment* algorithm aligns the display content to the appropriate position, and the *Lenticular Grating Segmentation* algorithm adjusts the image at the correct perceived depth based on the information captured by the depth camera. Together, these hardware and software components allow users to perceive AR content that seamlessly blends with mirror reflections, creating an engaging and immersive experience.

3.1 Binocular Disparity

We begin by giving a formal definition of binocular disparity in human vision. As depicted in Figure 4, consider a Cartesian coordinate system where the mirror is located on the $z = 0$ plane, and the origin is marked by the position of the depth camera. In this setup, the space with $z < 0$ is termed "mirror space," while the space where actual objects reside (also $z < 0$) is referred to as "real space." Let $E_{left} = (x_{left}, y_{left}, z_{left})$ denote the position of the user's left eye, and $E_{right} = (x_{right}, y_{right}, z_{right})$ the position of the right eye. Assume that point $P = (X, Y, Z)$ is an arbitrary point in real space, with $P' = (X, Y, -Z)$ representing its mirror reflection. The lines of sight from the left and right eyes to the reflection, denoted as vectors (E_{left}, P') and (E_{right}, P'), are distinct. This discrepancy in viewing angles constitutes binocular disparity and results in depth perception.

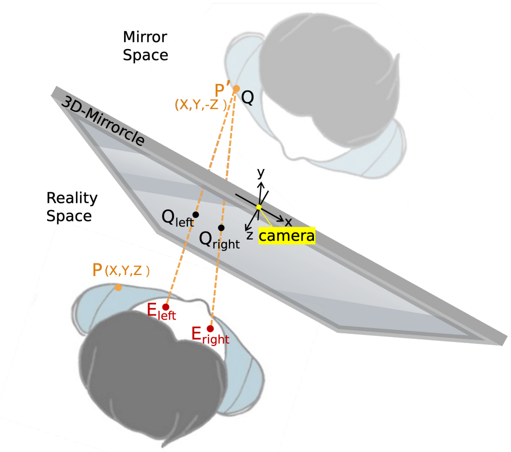

Fig. 4. Due to binocular disparity, each eye sees point P' from a distinct angle. To align point Q with P', we create parallax on the screen by showing points Q_{left} and Q_{right} at the sight-screen intersection, each visible to only one eye via lenticular grating, merging to create depth perception.

To display a point Q on the screen such that it visually overlaps with point P' from the viewer's perspective, the display must replicate the parallax effect. This involves two steps: (1) Separate point Q into two distinct points, Q_{left} and Q_{right}, corresponding to the viewer's left and right eyes, respectively. These points should be placed at the intersections of the viewer's lines of sight with the screen. (2) Employ a grating to direct Q_{left} exclusively to the left eye and Q_{right} exclusively to the right eye, ensuring that each eye perceives only its corresponding image. To achieve accurate alignment of the display in terms of both position and perceived depth, we employ a hardware-software co-design methodology to ensure precise coordination and visual processing.

3.2 Mirror Reflection Alignment (Position)

To determine the positions of Q_{left} and Q_{right} on the screen, we capture the pixel coordinates of human eyes using a color camera with a facial and body keypoint localization algorithm. These 2D coordinates are then transformed into 3D spatial coordinates with the depth camera's parameters. Lines extending from each eye to the mirror image point $P'(X, Y, -Z)$, representing real point $P(X, Y, Z)$, intersect the screen at points Q_{left} and Q_{right}, as shown in Figure 4. This ensures that point Q, as perceived by the observer, visually aligns with point P.

To compute the coordinates of Q_{left} on the screen, we establish a line from $E_{left}(x_{left}, y_{left}, z_{left})$ to the mirror image point $P'(X, Y, Z)$ We define this line using a parameter t_{left}. The parametric equation for this line is:

$$\begin{cases} x = x_{left} + t_{left}(X - x_{left}), \\ y = y_{left} + t_{left}(Y - y_{left}), \\ z = z_{left} + t_{left}(Z - z_{left}). \end{cases}$$

Setting z=0 for the intersection with the screen plane, we have

$$t_{left} = \frac{-z_{left}}{Z - z_{left}}.$$

Therefore, we can compute the coordinates of point Q_{left}:

$$Q_{left} = \left(x_{left} + t_{left} \cdot (X - x_{left}),\ y_{left} + t_{left} \cdot (Y - y_{left}),\ 0\right).$$

A similar approach is used to compute the coordinates of Q_{right}. Once we have established the spatial coordinates for both Q_{left} and Q_{right} relative to the depth camera at the origin, we adjust for the depth camera's position on the screen. Assuming thecamera's position at the screen's top, offset by dis_{camera} from the top-left corner, the screen coordinates are transformed to:

$$(Q_{left} + (dis_{camera}, 0, 0)) \cdot \theta,$$

where θ is the resolution conversion factor, and similarly for Q_{right}.

This transformation process aligns the virtual and real images by mapping each point on the mirror surface to its corresponding location on the screen, facilitating a real-time alignment of AR content to the mirror reflection.

3.3 Lenticular Grating Segmentation (Depth)

To ensure that each eye perceives only the intended image, we utilize a lenticular grating placed over the screen. The grating comprises parallel columns with consistent diameters, spacing, and heights, which cause light to diffract selectively for an interlaced display. This ensures each eye to view only half of the screen's pixels, separated into strips. The width of the strips that each eye views is governed by the grating's optical properties as described by the grating's imaging law, represented by the following equation [44, 60]:

$$f = \frac{r}{n-1}, \quad w = \frac{ef}{l-f}, \tag{1}$$

where f is the focal distance of the lenticular grating, r is the radius of curvature of the grating, n is the refractive index of the grating material, e is the distance of human eyes, l is the viewing distance, and w is the width of strips displayed on the screen. The left equation of (1) indicates that the focal length of the lenticular grating is determined by its curvature and the material's refractive index, affecting how light is focused to create distinct images for each eye. Subsequently, the right equation calculates the width of display strips visible to each eye, which depends on the eye's distance, the focal length of the grating, and the viewing distance, ensuring the correct parallax and depth perception.

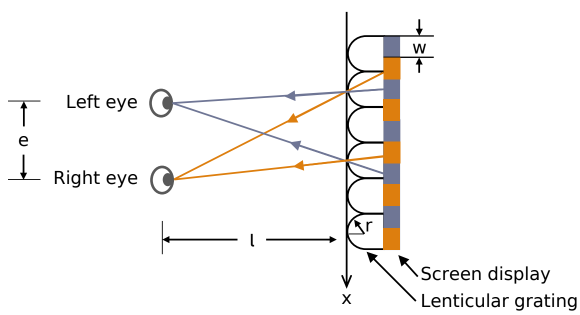

Fig. 5. The display is divided into interlaced strips. Through the refraction of a lenticular grating, the left eye can only see the blue strips, while the right eye can only see the orange strips.

Therefore, we can determine the central positions of the display stripes for the left and right eyes as the viewer's face moves:

$$x_l(m) = \frac{x_{left} + x_{right}}{2} + \frac{f \cdot (mT - \frac{1}{2}e)}{l - f} + mT,$$
$$x_r(m) = \frac{x_{left} + x_{right}}{2} + \frac{f \cdot (mT + \frac{1}{2}e)}{l - f} + mT, \tag{2}$$

where m represents the stripe index to be determined, T is the grating period, x_{left} and x_{right} are aforementioned human eye coordinates. As shown in Equation (2), when the hardware conditions are fixed, the position of the stripes is determined by the position of the human eyes and the distance l from the screen. Thus, as the integer m traverses the entire screen, we can obtain the central position of each stripe.

For point P', by employing Equation (2) and the pre-grating refraction coordinates of Q_{left} and Q_{right} in Section 3.2, we determine the specific m value, pinpointing the stripes displaying Q_{left} and Q_{right}. This calculation ensures that the left and right eyes perceive the intended parallax on the screen, aligning with point P'.

Note that when the viewer is positioned too close to the screen, the stripe width may exceed the inter-stripe spacing, leading to undesirable overlap of images meant for the left and right eyes. The images are displayed in alternating stripes on the screen. To ensure clear separation, the spacing between successive stripes for the same eye is given by:

$$x_l(m) - x_l(m-1) = \frac{Tl}{l - f},$$

where T denotes the grating period, l the viewing distance, and f the focal length of the lenticular grating. To prevent image crosstalk, where images for the left and right eyes merge, the spacing should satisfy:

$$\frac{Tl}{l - f} \geq \frac{2ef}{l - f}.$$

Thus, the minimum viewing distance l to avoid crosstalk is:

$$l \geq \frac{2ef}{T}.$$

Practically, to prevent displaying overly wide images that cause crosstalk, the pixel width on the screen is rounded down.

3.4 Prototype

For a more efficient and lightweight technical validation, we selected the Leia Lume Pad 2 as the display hardware [16]. The Lume Pad 2 features a well-manufactured lenticular sheet on the screen for 3D display, allowing for high-precision stereoscopic visual effects. Additionally, the Lume Pad 2 is equipped with a front-facing depth camera and a front-facing color camera, which enables direct binocular positioning and tracking.

The Lume Pad 2 is equipped with a Qualcomm Snapdragon 888 (2.8GHz) processor, an Adreno 660 GPU GPU, and 14GB of memory. We used the Leia Inc SDK [26] to develop a prototype, following Section 3.1 to 3.3. To achieve adaptive depth adjustment, we utilized the Lume Pad 2's built-in depth camera and implemented the MediaPipe [36] algorithm for recognizing and locating facial and body keypoints [1].

A half-mirror is then attached to the Lume Pad 2 to complete the 3D-Mirrorcle system setup, as shown in Figure 6.

[1] The software is developed as an Android application on the Lume Pad 2 and will be open-sourced upon acceptance.

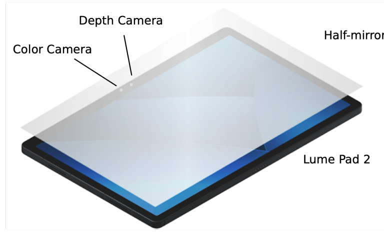

Fig. 6. The prototype of 3D-Mirrorcle consists of a Lume Pad 2 with a depth camera and a color camera, and a half-mirror.

4 EVALUATION

To comprehensively evaluate the advantages and disadvantages of 3D-Mirrorcle compared to existing smart mirror systems, we conducted a total of 4 experimental tasks. Task 1 & 2 are standardized tasks for measuring task completion accuracy and efficiency (Section 4.2). For Task 3 & 4, we built two applications to evaluate user experience in real-world scenarios (Section 4.3).

4.1 Participants and Procedure

We recruited 24 participants (10 males, 14 females), 21-37 years old ($M = 26.63$, $SD = 4.44$) [37], with normal or corrected-to-normal vision. The study lasted for ∼30 minutes per person, and each participant received a gift worth around US$5 upon completion of the experiment.

To simulate a real-world scenario where users may move during mirror use and are not equipped with additional devices, we compare the 3D-Mirrorcle system against 2D-optical and video-based smart mirror systems, which respectively serve as our baseline System A and B. Additional details about these systems are outlined in Table 1. Our user study setup is shown in Figure 7, with detailed information in Appendix Section 6.

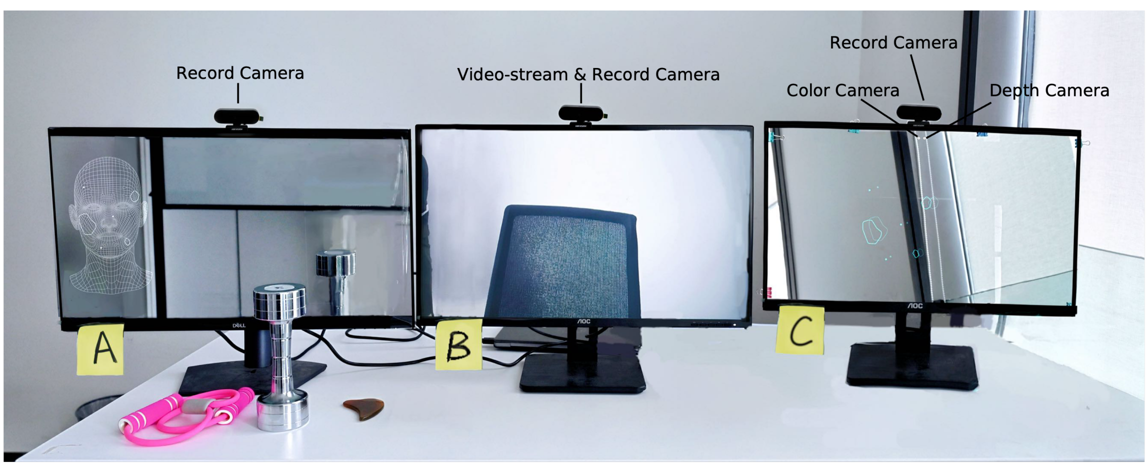

Fig. 7. Our user study setup. **System A** comprises a 2D display positioned behind a half-mirror, allowing users to view guidance images on the screen through the mirror. **System B** utilizes a camera that streams video to function as a pseudo-mirror, enabling users to see themselves alongside AR content in the video. **System C (3D-Mirrorcle)** integrates a 3D screen with a half-mirror to display two distinct images, one for each eye, which merge into a single depth-aligned 3D image from the viewer's perspective.

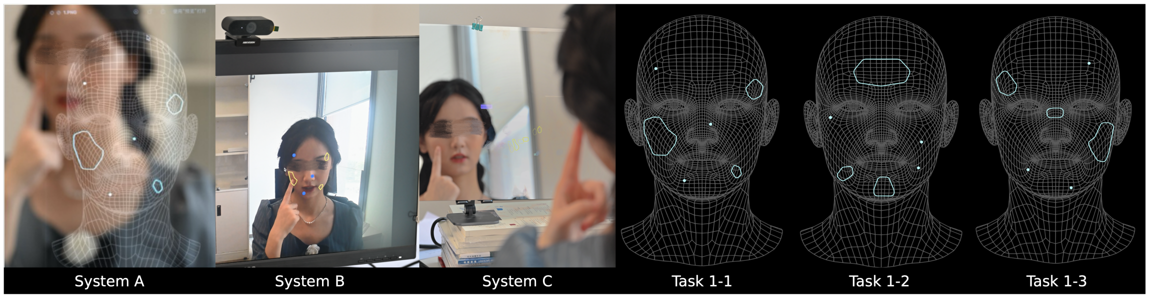

Fig. 8. Standardized Task 1: Participants use their fingertips to outline three circles and three points on their faces. Tasks 1-1, 1-2, and 1-3 rotate through three systems. In System C, though the images appear 2D, they create a 3D effect from the user's perspective, aligning with their face. Similar setups also apply to the other tasks.

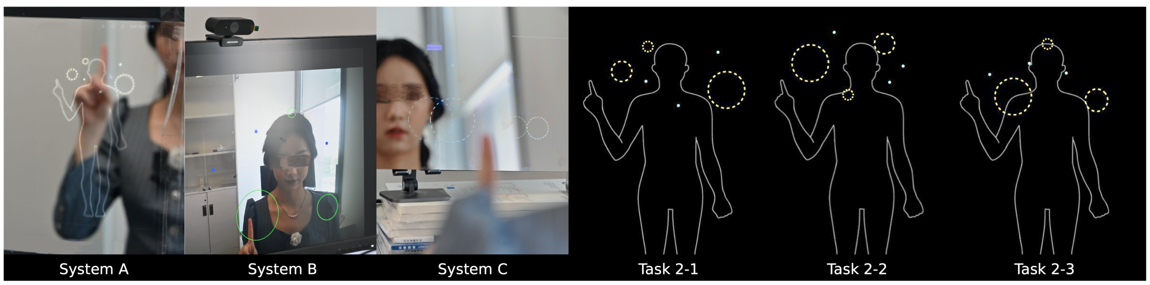

Fig. 9. Standardized Task 2: Participants are asked to trace circles in the air with their fingertips, which requires a broader range of movements than Task 1.

4.2 Standardized Tasks

We evaluated the effectiveness of 3D-Mirrorcle through standardized tasks designed to test precision and speed, comparing its performance against two baseline systems: a 2D-optical mirror system (System A) and a video-based system (System B). The study involved two specific tasks: Task 1 requires participants to outline their faces, while Task 2 involves air tracing. Each task required participants to draw three circles of varying sizes and three points, as illustrated in the images to the right of Figures 8 and 9.

Despite varying across the three systems, the difficulty levels of the tasks were maintained consistently, and the tasks and sequences were balanced and rotated among participants. Additionally, each participant completed a warm-up task using all three systems before proceeding to the main tasks.

We measured three objective metrics. **Area accuracy** was calculated using the Intersection-over-Union (IoU) ratio. This metric assesses the overlap between the users' drawn outlines and the predefined standard areas, adjusted for the camera's perspective. **Point distance** measures the deviation between the positions marked by the users' fingertips and the designated standard points. **Task completion time** is the total time taken by participants to draw the required circles and points, from the moment they viewed the display to the indication of task completion.

After each task, participants were also asked to complete a 7-point NASA TLX questionnaire [22] to evaluate the perceived workload associated with each task.

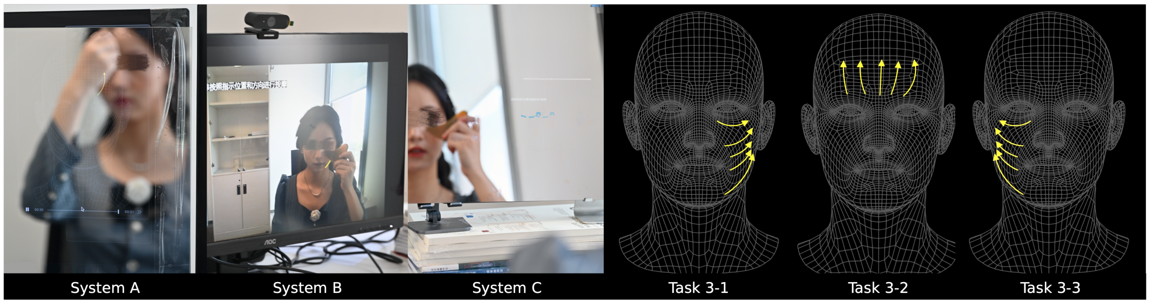

Fig. 10. Application Task 3 Setup: Participants are instructed to massage specific facial areas using a tool and essential oils.

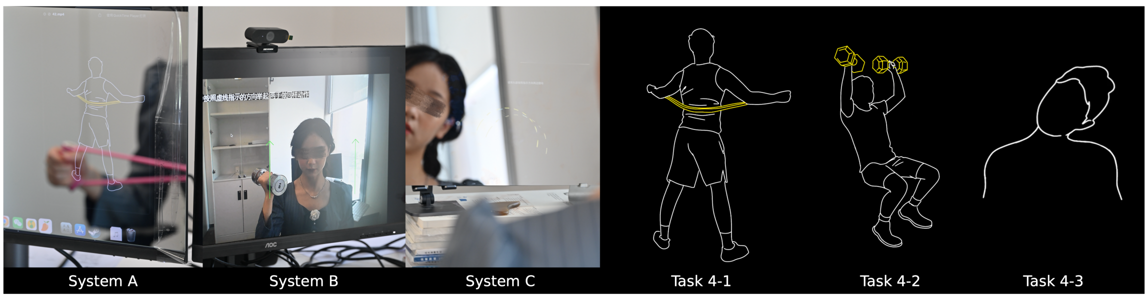

Fig. 11. Application Task 4 Setup: Participants are instructed to do physical exercises using fitness equipments, which involves dynamic full-body movements.

4.3 Application Tasks

To validate the generalizability of the system towards real-world use cases, we also designed two application scenarios to further assess 3D-Mirrorcle: facial massage (Task 3) and body workout (Task 4). The facial massage task was structured around three specific areas: left cheek, right cheek, and forehead. Participants experienced these areas sequentially across the three systems, performing a complete facial massage using essential oils and a massage tool. Similarly, the body workout scenario targeted three body parts: back, arms, and neck. Participants performed exercises using resistance bands and dumbbells on each of the three systems.

Following these practical tasks, we evaluated system usability using the System Usability Scale (SUS) questionnaire [7]. Additionally, we measured three supplementary dimensions: *Clarity*, *Comfort*, and *Immersion*, to provide a more comprehensive understanding of the user experience in real-world scenarios.

4.4 Evaluation Results

4.4.1 ***Enhanced Precision and Speed on Standardized Tasks.*** In both Task 1 & 2, 3D-Mirrorcle consistently outperformed the other systems, as shown in Figure 12 and 13,

Statistical analysis using Friedman tests [52, 70] confirmed significant differences among the systems for all measured metrics (all $p < 0.001$). Post-hoc Wilcoxon signed-rank tests [63] indicate that 3D-Mirrorcle was superior to

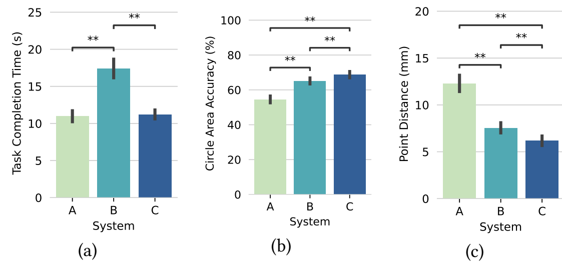

Fig. 12. Facial Outlining (Standardized Task 1) Objective Results. (a) Task completion time (s), (b) Circle area accuracy (%), and (c) Point distance (mm). Error bars represent 95% confidence intervals (CI). * stands for $p < 0.05$ and ** stands for $p < 0.01$. The same annotation applies to the rest of the paper. The results demonstrate that 3D-Mirrorcle exhibits a short task completion time and the highest accuracy in Task 1.

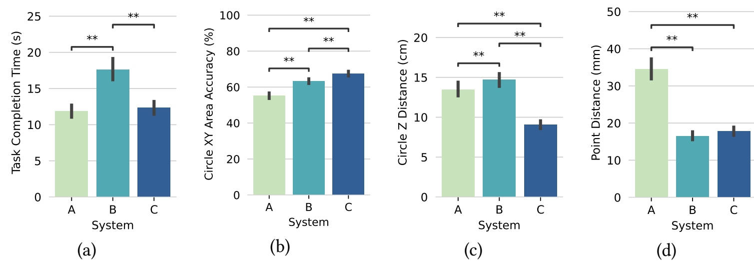

Fig. 13. Air Tracing (Standardized Task 2) objective results. (a) Task completion time (s), (b) Circle XY Area accuracy (%), (d) Circle Z distance (cm), and (d) Point distance (mm). The results show that 3D-Mirrorcle also demonstrates a short task completion time and the highest accuracy in tasks involving broader body movement.

System A in terms of area accuracy and point distance across both tasks (all $p < 0.001$). Against System B, 3D-Mirrorcle showed significant improvements in task completion time, area accuracy, and point distance in both tasks (all $p < 0.001$, except for point distance in Task 1, $p < 0.002$).

Specifically, in the air tracing task that involves a broader range of body movements (Task 2), 3D-Mirrorcle achieved an average z-axis distance of 9.08 cm ($SD = 3.01$), significantly outperforming System A's 13.46 cm ($SD = 5.21$) and System B's 14.7 cm ($SD = 4.88$). This demonstrates 3D-Mirrorcle's superior depth perception performance.

Overall, 3D-Mirrorcle offers the highest precision in standardized tasks, with users completing tasks both precisely and efficiently. In contrast, the 2D-optical setup (System A) relies on users glancing at diagrams and drawing circles with weak guidance, leading to a shorter task completion time but low accuracy. Users noted, *"System A has nothing to do with my face, it's just a hint"* (P5, 11). In the video-based setup (System B), the pseudo mirror obstructs users' ability to locate their fingers, resulting in longer task completion times but higher precision. User commented, *"The viewing angle of System B is a bit awkward"* (P12, 21). In contrast, 3D-Mirrorcle enables users to see themselves in a real mirror and simultaneously watch the guidance, facilitating both speed and accuracy. "In System C, I can find the specific positions quickly" (P9).

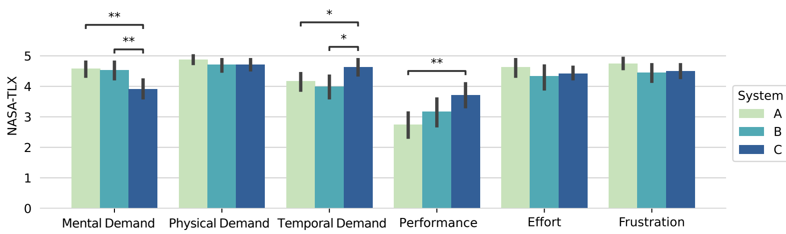

Fig. 14. Facial outlining (Standardized Task 1) NASA-TLX Results. Certain metrics were reversed for consistency, with higher scores indicating better outcomes. The results show that 3D-Mirrorcle significantly outperforms in temporal demand and performance, with a reasonable increase in mental demand.

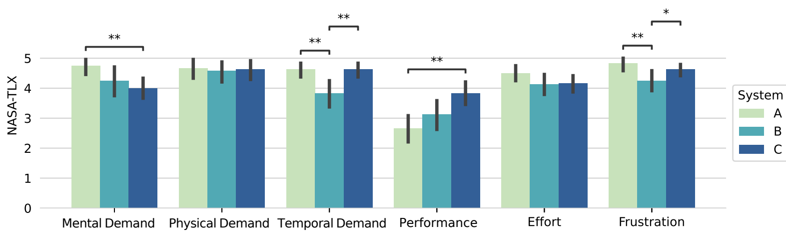

Fig. 15. Air Tracing (Standardized Task 2) NASA-TLX Results. Score interpretations are the same as Figure 14, and the results are similar.

4.4.2 ***Moderate Differences in Subjective Workloads.*** The workload results from the NASA-TLX questionnaire [22] in Task 1 and 2 are shown in Figure 14 and 15, where higher scores indicate better performance across all dimensions.

In both tasks, Friedman's tests revealed significant differences in mental demand, temporal demand, and performance. Subsequent post-hoc Wilcoxon signed-rank tests showed that 3D-Mirrorcle consistently outperformed in terms of temporal demand and performance, although it exhibited slightly worse in mental demands. Other dimensions did not show significant differences as per Friedman's tests.

The increased mental demand for 3D-Mirrorcle can be attributed to its novelty, in contrast to Systems A and B which users found more intuitive due to familiarity. Participant comments reflect this: System A was likened to "having a smartphone placed next to the mirror" (P3,7), System B to "the front camera of a smartphone" (P5), and System C as "new so I need to understand every time." (P19)

4.4.3 ***Improved User Experience on Application Tasks.*** In the evaluation of real-world applications, our system also demonstrated significant improvements in user experience across facial massage (Task 3) and body workout (Task 4), as shown in Figure 13 and 17. For the System Usability Scale (SUS), Friedman tests revealed significant differences across the three groups in both tasks. Post-hoc Wilcoxon signed-rank tests confirmed 3D-Mirrorcle 's significant improvements over System A ($p < 0.001$ for Task 3, $p = 0.019$ for Task 4), System B ($p < 0.001$ for Task 3 & 4).

The evaluation also extended to three additional dimensions of user experience in smart mirror tasks: Clarity, Comfort, and Immersion. Results from Friedman tests highlighted significant differences in clarity and immersion across all three systems (all $p < 0.01$), though no significant differences were found in comfort ($p = 0.067$ in task 3, $p = 0.089$ in task 4). Specifically, Wilcoxon signed-rank tests illustrated that clarity was significantly better than System B but

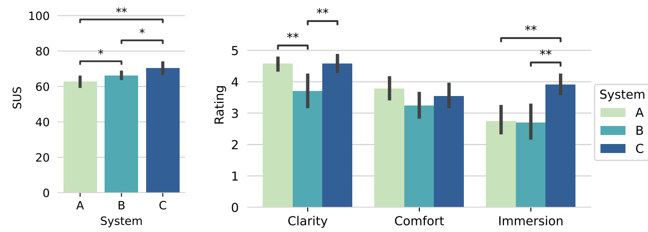

(a) (b)

Fig. 16. Facial Massage (Application Task 3) results: (a) SUS score (b) Clarity, comfort, and immersion ratings. The results demonstrate that 3D-Mirrorcle delivers superior system usability and immersion compared to baseline systems.

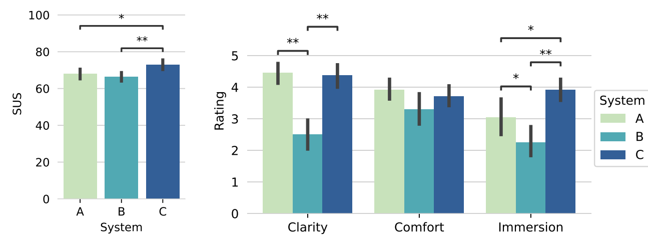

(a) (b)

Fig. 17. Body Workout (Application Task 4) results: (a) SUS score (b) Clarity, comfort, and immersion ratings. The results for Task 4 similarly highlight 3D-Mirrorcle 's strong performance in system usability and immersion.

comparable to System A, which is attributable to both System A and C utilizing real mirrors, whereas System B employs a pseudo mirror. Moreover, 3D-Mirrorcle significantly improved users' sense of immersion compared to both System A and System B (all $p < 0.001$), reflecting deeper engagement in the interactions. Users noted, "System A is like the information floating on the surface" (P2, 23) and "System B makes me feel in another world, maybe because it is from an upper viewing angle" (P17). In contrast, 3D-Mirrorcle immerses users by displaying content within the realistic space of a mirror, as users observed, "I feel like the information is in the same space as me" (P5,24).

These results collectively indicate that 3D-Mirrorcle not only streamlines task completion at a fundamental level but also significantly boosts user satisfaction in real-world applications.

4.4.4 ***High Overall Satisfaction Rating.*** Following the completion of all four task tasks, we surveyed users regarding their overall satisfaction, asking them to rank the three systems. The results, displayed in Figure 18, show that System C (3D-Mirrorcle) received the highest number of first-place rankings and the fewest third-place rankings.

5 DISCUSSION

5.1 Potential Applications

The application scenarios dictate how the 3D-Mirrorcle technology integrates into people's daily lives. After user experiments, we also solicited feedback on potential application scenarios other than facial massage and exercise fitness. The summarized applications are depicted in Figure 19.

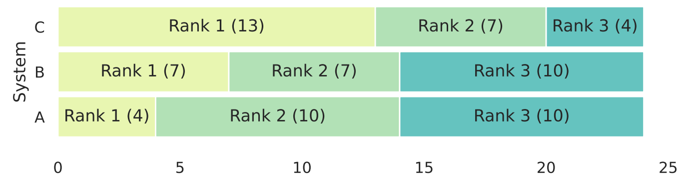

Fig. 18. Overall Satisfaction ranking based on the user experience on four tasks. Over half of the participants (13 out of 24) ranked 3D-Mirrorcle as their top choice.

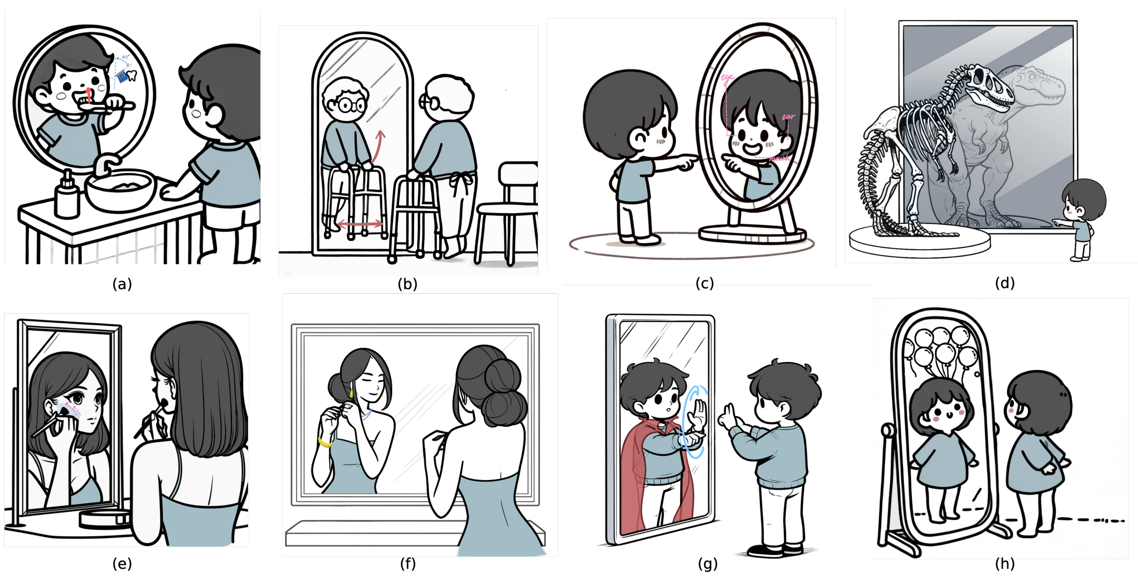

Fig. 19. Other potential applications of 3D-Mirrorcle: (a) Personal hygiene, (b) Elderly rehabilitation, (c) Embodied education, (d) Exhibition display, (e) Makeup guidance, (f) Jewelry try-on, (g) Interaction game, (h) Fun effects.

Personal Hygiene: 3D-Mirrorcle can be integral to personal hygiene routines by offering reminders and visual guidance for tasks like teeth brushing, hand washing, and skin care routines.

Elderly Rehabilitation: Our system facilitates elderly rehabilitation by providing tailored exercise routines with real-time feedback and safety monitoring through sensors to improve mobility and strength.

Embodied Education: The immersive nature of our system makes it a powerful tool in embodied learning, assisting in activities like identifying body parts, interactive language learning, or history lessons about ancient civilizations.

Exhibition Display: 3D-Mirrorcle can transform exhibition spaces into dynamic, interactive environments. Visitors can engage with exhibits through AR that provides additional information, interactive timelines, or even virtual guided tours, enhancing the educational value and engagement of museum visits.

Makeup Guidance: Our system is ideal for makeup application, where precision and depth perception are crucial. AR technology enhances the experience by providing real-time guidance and visual overlays.

Jewelry Try-On: Our system allows users to virtually try on pieces of jewelry, viewing them from various angles with realistic depth effects, thereby aiding in better decision-making at home and enhancing the shopping experience for luxury goods.

Interactive Gaming: Leveraging its interactive capabilities, our system supports games that respond to gestures and voice commands, offering immersive experiences like virtual outfit changes, house building, or competing with virtual or real opponents.

Fun Effects: 3D-Mirrorcle can also be used for creating fun effects in video calls, social media, or during live events. Users can apply real-time filters, backgrounds, and animations that respond to their movements and expressions.

5.2 Future Enhancement of the System

Multi-User Support: The current specifications of the half-mirror and grating limit the viewing experience to single users, precluding simultaneous multi-user interaction. Future research can investigate multi-viewpoint tracking, possibly through the use of spherical gratings, to enable multi-user engagement.

Adaptive Reflectance and Transparency: The fixed reflectance of the half-mirror hinders seamless AR integration, preventing a complete overlay akin to existing AR technologies. Future research into photochromic glass, capable of dynamically altering its transparency, may facilitate smoother transitions between overlay and replacement effects.

Privacy Safeguarding: The use of cameras for data capture in 3D-Mirrorcle raises privacy issues. To mitigate these risks, implementing physical camera shutters and enhancing data security with encryption methods is essential for safeguarding user privacy.

New Software Market and Generative AI: Future extensions of 3D-Mirrorcle could leverage generative AI to enhance user interaction and personalization, which opens the potential for new software markets in areas like education and healthcare. By integrating AI-driven content generation, the system could offer tailored information overlays like health analytics and personalized fitness coaching. Additionally, improving gesture and voice recognition capabilities could make the interface more intuitive. This would not only boost user engagement but also expand the practical applications of smart mirrors in daily and professional environments.

5.3 Limitations

While 3D-Mirrorcle marks a significant advancement in depth-enhanced mirror displays, it faces several limitations that highlight the need for further research and development. The system requires users to undergo a considerable period of acclimatization due to its unique display, which integrates augmented reality effects with reflections, suggesting that improvements are needed to enhance ease of use. Additionally, the relatively brief evaluation period may not adequately capture long-term usability or the full user experience, particularly as the evaluation does not completely address all three-dimensional interactions, which could limit our understanding of its performance in real-world scenarios. Furthermore, the higher cost of the required hardware poses challenges for widespread consumer adoption, with concerns about accessibility, scalability, and the durability of the system for daily use also yet to be fully addressed.

6 CONCLUSION

We presented 3D-Mirrorcle, an innovative system capable of rendering depth-tracking AR effects in a mirror setting. To mitigate binocular disparity and create glasses-free depth perception, we carried out a hardware-software co-design, which includes a *Mirror Reflection Alignment* algorithm to ensure accurate positioning and a *Lenticular Grating Segmentation* algorithm to achieve dynamic depth adjustment. Through extensive user studies, our system demonstrates superior task completion accuracy and efficiency, enhanced usability and immersion, and improved overall satisfaction compared to the existing systems. It has potential in various applications like healthcare, education, gaming, and exhibitions, which could significantly impact people's daily lives.

ACKNOWLEDGMENTS

REFERENCES

[1] Dabiah A Alboaneen, Dalia Alsaffar, Alyah Alateeq, Amani Alqahtani, Amjad Alfahhad, Bashaier Alqahtani, Rahaf Alamri, and Lama Alamri. 2020. Internet of things based smart mirrors: A literature review. In *2020 3rd International Conference on Computer Applications & Information Security (ICCAIS)*. IEEE, 1–6.

[2] Fraser Anderson, Tovi Grossman, Justin Matejka, and George Fitzmaurice. 2013. YouMove: enhancing movement training with an augmented reality mirror. In *Proceedings of the 26th annual ACM symposium on User interface software and technology*. 311–320.

[3] S Athira, Frangly Francis, Radwin Raphel, NS Sachin, Snophy Porinchu, and Seenia Francis. 2016. Smart mirror: A novel framework for interactive display. In *2016 International conference on circuit, power and computing technologies (ICCPCT)*. IEEE, 1–6.

[4] Daniel Besserer, Johannes Bäurle, Alexander Nikic, Frank Honold, Felix Schüssel, and Michael Weber. 2016. Fitmirror: a smart mirror for positive affect in everyday user morning routines. In *Proceedings of the workshop on multimodal analyses enabling artificial agents in human-machine interaction*. 48–55.

[5] Oliver Bimber and Ramesh Raskar. 2005. *Spatial augmented reality: merging real and virtual worlds*. CRC press.

[6] Tobias Blum, Valerie Kleeberger, Christoph Bichlmeier, and Nassir Navab. 2012. mirracle: An augmented reality magic mirror system for anatomy education. In *2012 IEEE Virtual Reality Workshops (VRW)*. IEEE, 115–116.

[7] J Brooke. 1996. SUS: A quick and dirty usability scale. *Usability Evaluation in Industry* (1996).

[8] Alex Butler, Otmar Hilliges, Shahram Izadi, Steve Hodges, David Molyneaux, David Kim, and Danny Kong. 2011. Vermeer: direct interaction with a 360 viewable 3D display. In *Proceedings of the 24th annual ACM symposium on User interface software and technology*. 569–576.

[9] Julie Carmigniani, Borko Furht, Marco Anisetti, Paolo Ceravolo, Ernesto Damiani, and Misa Ivkovic. 2011. Augmented reality technologies, systems and applications. *Multimedia tools and applications* 51 (2011), 341–377.

[10] Sara Colantonio, Giuseppe Coppini, Daniela Germanese, Daniela Giorgi, Massimo Magrini, Paolo Marraccini, Massimo Martinelli, Maria Aurora Morales, Maria Antonietta Pascali, Giovanni Raccichini, et al. 2015. A smart mirror to promote a healthy lifestyle. *Biosystems Engineering* 138 (2015), 33–43.

[11] Oliver S Cossairt, Joshua Napoli, Samuel L Hill, Rick K Dorval, and Gregg E Favalora. 2007. Occlusion-capable multiview volumetric three-dimensional display. *Applied optics* 46, 8 (2007), 1244–1250.

[12] James E Cutting. 1997. How the eye measures reality and virtual reality. *Behavior Research Methods, Instruments, & Computers* 29, 1 (1997), 27–36.

[13] Chi Tai Dang, Ilhan Aslan, Florian Lingenfelser, Tobias Baur, and Elisabeth André. 2019. Towards somaesthetic smarthome designs: Exploring potentials and limitations of an affective mirror. In *Proceedings of the 9th International Conference on the Internet of Things*. 1–8.

[14] Jean Baptiste De la Riviere, Nicolas Dittlo, Emmanuel Orvain, Cédric Kervégant, and Mathieu Courtois. 2010. Holocubtile: 3D multitouch brings the virtual world into the user's hands. In *ACM International Conference on Interactive Tabletops and Surfaces*. 311–311.

[15] Tomohiro Endo, Yoshihiro Kajiki, Toshio Honda, and Makoto Sato. 2000. Cylindrical 3-D video display observable from all directions. In *Proceedings the Eighth Pacific Conference on Computer Graphics and Applications*. IEEE, 300–306.

[16] David Fattal. 2021. LEIA: The Lume Pad: 3D Lightfield at your fingertips. In *SPIE AVR21 Industry Talks II*, Vol. 11764. SPIE, 1176415.

[17] Jason Geng. 2013. Three-dimensional display technologies. *Advances in optics and photonics* 5, 4 (2013), 456–535.

[18] Stevie Giovanni, Yeun Chul Choi, Jay Huang, Eng Tat Khoo, and KangKang Yin. 2012. Virtual try-on using kinect and HD camera. In *Motion in Games: 5th International Conference, MIG 2012, Rennes, France, November 15-17, 2012. Proceedings 5*. Springer, 55–65.

[19] Oihane Gomez-Carmona and Diego Casado-Mansilla. 2017. SmiWork: An interactive smart mirror platform for workplace health promotion. In *2017 2nd International Multidisciplinary Conference on Computer and Energy Science (SpliTech)*. IEEE, 1–6.

[20] Umut Gültepe and Uğur Güdükbay. 2014. Real-time virtual fitting with body measurement and motion smoothing. *Computers & Graphics* 43 (2014), 31–43.

[21] Martin Hachet, Benoit Bossavit, Aurélie Cohé, and Jean-Baptiste de La Rivière. 2011. Toucheo: multitouch and stereo combined in a seamless workspace. In *Proceedings of the 24th annual ACM symposium on User interface software and technology*. 587–592.

[22] Sandra G Hart and Lowell E Staveland. 1988. Development of NASA-TLX (Task Load Index): Results of empirical and theoretical research. In *Advances in psychology*. Vol. 52. Elsevier, 139–183.

[23] Otmar Hilliges, David Kim, Shahram Izadi, Malte Weiss, and Andrew Wilson. 2012. HoloDesk: direct 3d interactions with a situated see-through display. In *Proceedings of the SIGCHI Conference on Human Factors in Computing Systems*. 2421–2430.

[24] Akpa Akpro Elder Hippocrate, Edith Talina Luhanga, Takata Masashi, Ko Watanabe, and Keiichi Yasumoto. 2017. Smart gyms need smart mirrors: design of a smart gym concept through contextual inquiry. In *Proceedings of the 2017 ACM International Joint Conference on Pervasive and Ubiquitous Computing and Proceedings of the 2017 ACM International Symposium on Wearable Computers*. 658–661.

[25] Tianqi Huang, Boxuan Han, Xinran Zhang, and Hongen Liao. 2019. High-performance autostereoscopic display based on the lenticular tracking method. *Optics express* 27, 15 (2019), 20421–20434.

[26] Leia Inc. 2024. Leia Core Native SDK (CNSDK) Documentation. https://leiainc.github.io/CNSDK-Doxygen-Documentation/index.html.

[27] Haruo Isono, Minoru Yasuda, Daisuke Takemori, Hideyuki Kanayama, Chihiko Yamada, and Kazuaki Chiba. 1992. 50-inch autostereoscopic full-color 3D TV display system. In *Stereoscopic Displays and Applications III*, Vol. 1669. SPIE, 176–185.

[28] Frederic E Ives. 1902. A novel stereogram. *Journal of the Franklin Institute* 153, 1 (1902), 51–52.

[29] Andrew Jones, Ian McDowall, Hideshi Yamada, Mark Bolas, and Paul Debevec. 2007. Rendering for an interactive 360 light field display. In *ACM SIGGRAPH 2007 papers*. 40–es.

[30] Michael W Jones, Gregory P Nordin, Jeffrey H Kulick, Robert G Lindquist, and Stephen T Kowel. 1995. Liquid crystal display based implementation of a real-time ICVision holographic stereogram display. In *Practical Holography IX*, Vol. 2406. SPIE, 154–164.

[31] Hojoong Kim, Young-Tae Kwon, Hyo-Ryoung Lim, Jong-Hoon Kim, Yun-Soung Kim, and Woon-Hong Yeo. 2021. Recent advances in wearable sensors and integrated functional devices for virtual and augmented reality applications. *Advanced Functional Materials* 31, 39 (2021), 2005692.

[32] Gun A Lee, Hye Sun Park, and Mark Billinghurst. 2019. Optical-reflection type 3d augmented reality mirrors. In *Proceedings of the 25th ACM symposium on virtual reality software and technology*. 1–2.

[33] Gun A Lee, Hye Sun Park, Seungwon Kim, and Mark Billinghurst. 2020. Improving User Experience in Augmented Reality Mirrors with 3D Displays. In *Advances in Visual Computing: 15th International Symposium, ISVC 2020, San Diego, CA, USA, October 5–7, 2020, Proceedings, Part I 15*. Springer, 642–653.

[34] Joon Hyub Lee, Seok-Hyung Bae, Jinyung Jung, and Hayan Choi. 2012. Transparent display interaction without binocular parallax. In *Adjunct proceedings of the 25th annual ACM symposium on User interface software and technology*. 97–98.

[35] Yejun Liu, Jia Jia, Jingtian Fu, Yihui Ma, Jie Huang, and Zijian Tong. 2016. Magic mirror: A virtual fashion consultant. In *Proceedings of the 24th ACM international conference on Multimedia*. 680–683.

[36] Camillo Lugaresi, Jiuqiang Tang, Hadon Nash, Chris McClanahan, Esha Uboweja, Michael Hays, Fan Zhang, Chuo-Ling Chang, Ming Guang Yong, Juhyun Lee, et al. 2019. Mediapipe: A framework for building perception pipelines. *arXiv preprint arXiv:1906.08172* (2019).

[37] Ritch Macefield. 2009. How to specify the participant group size for usability studies: a practitioner's guide. *Journal of usability studies* 5, 1 (2009), 34–45.

[38] Federico Manuri, Andrea Sanna, et al. 2016. A survey on applications of augmented reality. *ACSIJ Advances in Computer Science: an International Journal* 5, 1 (2016), 18–27.

[39] Marco Marcon, Augusto Sarti, and Stefano Tubaro. 2016. Toothbrush motion analysis to help children learn proper tooth brushing. *Computer Vision and Image Understanding* 148 (2016), 34–45.

[40] Diego Martinez Plasencia, Florent Berthaut, Abhijit Karnik, and Sriram Subramanian. 2014. Through the combining glass. In *Proceedings of the 27th annual ACM symposium on User interface software and technology*. 341–350.

[41] Willem A Melder, Khiet P Truong, Marten Den Uyl, David A Van Leeuwen, Mark A Neerincx, Lodewijk R Loos, and B Stock Plum. 2007. Affective multimodal mirror: sensing and eliciting laughter. In *Proceedings of the international workshop on Human-centered multimedia*. 31–40.

[42] Akeem Olowolayemo, Saleh Alenazi, and Faten Anis Syairah Seri. 2018. Mirror that Talks: A Self-Motivating Personal Vision Assistant. In *Proceedings of the 2018 International Conference on Image and Graphics Processing*. 157–161.

[43] Katsuyuki Omura, Shinichi Shiwa, and Tsutomu Miyasato. 1998. Lenticular autostereoscopic display system: multiple images for multiple viewers. *Journal of the Society for Information Display* 6, 4 (1998), 313–324.

[44] Daechul Park, Kyungtae Kim, Cheonhee Lee, Jungyoung Son, and Yongbeom Lee. 1995. Lenticular stereoscopic imaging and displaying techniques with no special glasses. In *Proceedings., International Conference on Image Processing*, Vol. 3. IEEE, 137–140.

[45] Siegmund Pastoor and Matthias Wöpking. 1997. 3-D displays: A review of current technologies. *Displays* 17, 2 (1997), 100–110.

[46] Cristina Portalés, Jesús Gimeno, Sergio Casas, Ricardo Olanda, and Francisco Giner Martínez. 2018. Interacting with augmented reality mirrors. In *Virtual and Augmented Reality: Concepts, Methodologies, Tools, and Applications*. IGI Global, 18–46.

[47] Timothy Poston and Luis Serra. 1994. The virtual workbench: Dextrous VR. In *Virtual reality software and technology*. World Scientific, 111–121.

[48] Nils-Christian W Rabben and Stine Aurora Mikkelsplass. 2021. A smart mirror to encourage independent hand washing for children. In *Human Interaction, Emerging Technologies and Future Applications IV: Proceedings of the 4th International Conference on Human Interaction and Emerging Technologies: Future Applications (IHIET–AI 2021), April 28-30, 2021, Strasbourg, France 4*. Springer, 447–456.

[49] Stephan Reichelt, Ralf Häussler, Gerald Fütterer, and Norbert Leister. 2010. Depth cues in human visual perception and their realization in 3D displays. In *Three-Dimensional Imaging, Visualization, and Display 2010 and Display Technologies and Applications for Defense, Security, and Avionics IV*, Vol. 7690. SpIE, 92–103.

[50] Andrea Salgian, David Vickerman, and David Vassallo. 2017. A smart mirror for music conducting exercises. In *Proceedings of the on Thematic Workshops of ACM Multimedia 2017*. 544–549.

[51] Ian Sexton and Phil Surman. 1999. Stereoscopic and autostereoscopic display systems. *IEEE Signal Processing Magazine* 16, 3 (1999), 85–99.

[52] Michael R Sheldon, Michael J Fillyaw, and W Douglas Thompson. 1996. The use and interpretation of the Friedman test in the analysis of ordinal-scale data in repeated measures designs. *Physiotherapy Research International* 1, 4 (1996), 221–228.

[53] Jung-Young Son, Vladmir V Saveljev, Yong-Jin Choi, Ji-Eun Bahn, Sung-Kyu Kim, and Hyunhee Choi. 2003. Parameters for designing autostereoscopic imaging systems based on lenticular, parallax barrier, and integral photography plates. *Optical Engineering* 42, 11 (2003), 3326–3333.

[54] Sopicha Stirapongsasuti, Kundjanasith Thonglek, Shinya Misaki, Yugo Nakamura, and Keiichi Yasumoto. 2021. Insha: Intelligent nudging system for hand hygiene awareness. In *Proceedings of the 21st ACM International Conference on Intelligent Virtual Agents*. 183–190.

[55] Toshiki Toda, Susumu Takahashi, and Fujio Iwata. 1995. Three-dimensional (3D) video system using grating image. In *Practical Holography IX*, Vol. 2406. SPIE, 191–198.

[56] Hakan Urey, Kishore V Chellappan, Erdem Erden, and Phil Surman. 2011. State of the art in stereoscopic and autostereoscopic displays. *Proc. IEEE* 99, 4 (2011), 540–555.

[57] Keita Ushida, Yu Tanaka, Takeshi Naemura, and Hiroshi Harashima. 2002. i-mirror: An interaction/information environment based on a mirror metaphor aiming to install into our life space. In *Proceedings of the 12th International Conference on Artificial Reality and Telexistence (ICAT2002)*. 113–118.

[58] Cees Van Berkel and John A Clarke. 1997. Characterization and optimization of 3D-LCD module design. In *Stereoscopic Displays and Virtual Reality Systems IV*, Vol. 3012. SPIE, 179–186.

[59] Cees Van Berkel, David W Parker, and Anthony R Franklin. 1996. Multiview 3D LCD. In *Stereoscopic displays and virtual reality systems III*, Vol. 2653. SPIE, 32–39.

[60] Ai-Hong Wang, Qiong-Hua Wang, Xiao-Fang Li, and Da-Hai Li. 2012. Combined lenticular lens for autostereoscopic three dimensional display. *Optik* 123, 9 (2012), 827–830.

[61] Kaixuan Wang, Lim Wei Yap, Shu Gong, Ren Wang, Stephen Jia Wang, and Wenlong Cheng. 2021. Nanowire-based soft wearable human–machine interfaces for future virtual and augmented reality applications. *Advanced Functional Materials* 31, 39 (2021), 2008347.

[62] Mark Weiser. 1999. The computer for the 21st century. *ACM SIGMOBILE mobile computing and communications review* 3, 3 (1999), 3–11.

[63] Frank Wilcoxon, S Katti, Roberta A Wilcox, et al. 1970. Critical values and probability levels for the Wilcoxon rank sum test and the Wilcoxon signed rank test. *Selected tables in mathematical statistics* 1 (1970), 171–259.

[64] Graham J Woodgate, David Ezra, Jonathan Harrold, Nicolas S Holliman, Graham R Jones, and Richard R Moseley. 1997. Observer-tracking autostereoscopic 3D display systems. In *Stereoscopic Displays and Virtual Reality Systems IV*, Vol. 3012. SPIE, 187–198.

[65] Graham J Woodgate, Jonathan Harrold, Adrian MS Jacobs, Richard R Moseley, and David Ezra. 2000. Flat-panel autostereoscopic displays: characterization and enhancement. In *Stereoscopic displays and virtual reality systems VII*, Vol. 3957. SPIE, 153–164.

[66] Rui-Ping Yang, Zhen-Tao Liu, Li-Dong Zheng, Jia-Peng Wu, and Cong-Cong Hu. 2018. Intelligent mirror system based on facial expression recognition and color emotion adaptation——iMirror. In *2018 37th Chinese Control Conference (CCC)*. IEEE, 3227–3232.

[67] Yuan-Chih Yu, Shingchern D You, and Dwen-Ren Tsai. 2012. Magic mirror table for social-emotion alleviation in the smart home. *IEEE Transactions on Consumer Electronics* 58, 1 (2012), 126–131.

[68] Yanxiang Zhang and Zhenxing Zhang. 2020. A comparative study of the influence of the screen size of mobile devices on the experience effect of 3D content in the form of AR/VR technology. In *Augmented Reality, Virtual Reality, and Computer Graphics: 7th International Conference, AVR 2020, Lecce, Italy, September 7–10, 2020, Proceedings, Part I 7*. Springer, 363–374.

[69] Jun Zhuang, Yue Liu, Yanyang Jia, and Yisong Huang. 2019. User discomfort evaluation research on the weight and wearing mode of head-wearable device. In *Advances in Human Factors in Wearable Technologies and Game Design: Proceedings of the AHFE 2018 International Conferences on Human Factors and Wearable Technologies, and Human Factors in Game Design and Virtual Environments, Held on July 21–25, 2018, in Loews Sapphire Falls Resort at Universal Studios, Orlando, Florida, USA 9*. Springer, 98–110.

[70] Donald W Zimmerman and Bruno D Zumbo. 1993. Relative power of the Wilcoxon test, the Friedman test, and repeated-measures ANOVA on ranks. *The Journal of Experimental Education* 62, 1 (1993), 75–86.

APPENDIX A: SUPPLEMENTARY EXPERIMENTAL SETUPS

In the experimental setup for the 3D-Mirrorcle, participants were positioned within 10 cm to 80 cm from the mirror, with an optimal viewing distance averaging around 40 cm. Display brightness settings were adjusted to 450 nits for 2D content (System A and B) and 300 nits for 3D content (System C) to optimize visibility. Cameras with a resolution of 3264×2040 pixels were mounted on the display of three systems at the same position to capture data for evaluation. A perspective transformation approach was employed in the computation of Intersection over Union (IoU) metrics to guarantee the accuracy of the camera's perspective relative to the human eye. Additionally, the target circles in standardized tasks were set independently for each participant, ensuring consistency across individual experiences.

Received xxx xxx xxxx; revised xxx xxx xxxx; accepted xxx xxx xxxx